Hydrogeochemical characteristics and source identification of salinity in groundwater resources in an arid plain, northeast of Iran: implication for drinking and irrigation purposes

Caratteristiche idrogeochimiche ed identificazione dell'origine della salinità nelle risorse idriche sotterranee di una pianura arida dell'Iran nord-orientale: implicazioni per scopi irrigui ed idropotabili

Parisan Taherian[a], Ata Joodavi[b] ✍

[a]Department of Water Engineering, Faculty of Agriculture, Ferdowsi University, Mashhad, Iran - email: *parisantaheri@gmail.com*
[b]Department of Water Engineering, Kashmar Higher Education Institute, Kashmar, Iran ✍ email: *atajoodavi@kashmar.ac.ir; atajoodavi@gmail.com*

Citation:
Joodavi A, Taherian P (2021) Hydrogeochemical characteristics and source identification of salinity in groundwater resources in an arid plain, northeast of Iran: implication for drinking and irrigation purposes. Acque Sotterranee - *Italian Journal of Groundwater*, 10(2), 21 - 31 https://doi.org/10.7343/as-2021-502

Correspondence to:
Ata Joodavi ✍
atajoodavi@kashmar.ac.ir
atajoodavi@gmail.com

Riassunto

La salinizzazione delle acque sotterranee è una problematica comune a molte aree del mondo dove queste acque rappresentano la principale risorsa idropotabile. Questo lavoro combina un approccio geochimico e statistico per analizzare i meccanismi che influenzano la chimica delle acque sotterranee ospitate nell'acquifero di Neyshabour (Iran nord-orientale) e l'origine dei sali disciolti. I valori medi di Mg^{2+} (61.4 mg/L), Na^+ (553.2 mg/L), Cl^- (800.4 mg/L), SO_4^{2-} (428.7 mg/L), EC (3404 µS/cm), TH (525.0 mg/L) e TDS (2212.8 mg/L) calcolati da 55 campioni di acqua campionati in pozzi profondi sono risultati superiori rispetto ai valori di riferimento suggeriti dalle direttive WHO e ISIRI. I risultati dell'analisi geochimica e di un analisi statistica multivariata suggeriscono che: i) l'assetto geologico influenza il quantitativo di sali disciolti, e ii) acque clorurato-sodiche e bicarbonato-sodiche sono preponderanti nell'area di studio. Oltre all'interazione acqua-roccia (e.g. dissoluzione di evaporiti), l'infiltrazione di acque irrigue e l'abbassamento della tavola d'acqua hanno incrementato la salinità delle acque nell'acquifero di Neyshabour. Il dilavamento di rocce mafiche ed ultramafiche di complessi ofiolitici è responsabile dell'arricchimento di Mg^{2+} nella maggior parte dei campioni. L'indice di qualità dell'acqua (WQI) e altri indici suggeriscono che le acque sotterranee sono generalmente di scarsa qualità per scopi idropotabili ed irrigui in particolar modo nella parte meridionale, centrale ed occidentale della pianura.

Abstract

Groundwater salinization is a worldwide problem where groundwater is the principal source of water. A combination of geochemical and statistical approaches was used to investigate the mechanisms governing the groundwater chemistry and origin of salts in the Neyshabour aquifer (north-eastern Iran). The mean values of Mg^{2+} (61.4 mg/L), Na^+ (553.2 mg/L), Cl^- (800.4 mg/L), SO_4^{2-} (428.7 mg/L), EC (3404 µS/cm), TH (525.0 mg/L) and TDS (2212.8 mg/L) in 55 groundwater samples taken from deep wells were higher than WHO and ISIRI guideline values. Geochemical and multivariate statistical analysis suggested that: i) the dissolved solids in the water samples are controlled mainly by geology, and ii) Na-Cl and Na-HCO$_3$ type waters are dominant in the area. Besides the water–rock reactions (e.g., evaporites dissolution), groundwater salinity in Neyshabour aquifer has been intensified by irrigation return flows and groundwater level decline. The chemical weathering of mafic and ultramafic rocks in ophiolitic rocks is responsible for Mg enrichment in the majority of samples. Water quality index (WQI) and different indices calculated for the groundwater samples indicated that the most of them have poor water quality for drinking and agricultural uses especially in the southern, central and western parts of the plain.

Inroduction

Groundwater provides a reliable water supply source especially in arid and semi-arid regions (Joodavi et al. 2020). However, natural and anthropogenic factors could deteriorate chemical characteristics of groundwater resources that make them unsuitable for human consumption (Herojeet et al. 2020). Globally, the most common recognized salt sources in groundwater include evaporation, mobilization of unsaturated-zone salts, evaporate leaching, marine saltwater intrusion, infiltration of polluted non-marine surface waters, highly mineralized water from geothermal fields, sea spray, agricultural practices and the wetting and drying cycles (Richter and Kreitler 1993; Giambastiani et al. 2013; Mirzavand et al. 2020, Pauloo et al. 2021).

Groundwater is the primary source of water used for irrigation and domestic and industrial water supply in Iran. It has been indicated that investigations on the hydrogeochemical evolution of groundwater resources are essential for sustainable development in developing countries such as Iran (Sheikhy Narany et al. 2014). Until now, no comprehensive research is available on the hydrogeochemical characteristics of groundwater in the Neyshabour Plain located in north-eastern Iran. In our study, it was intended to provide an insight of factors controlling the chemistry and salinization of groundwater in Neyshabour Plain and to evaluate the suitability of groundwater quality for irrigation and drinking purposes.

Study area

The Neyshabour watershed is located in Razavi Khorasan province in the northeast of Iran (Fig. 1). The study area has semi-arid to arid climate conditions with average annual precipitation of 249.1 mm and annual potential evapotranspiration of about 2,335 mm. The maximum and minimum elevations in the watershed are 3,300 m and 1,050 m above the mean sea level in Binalood Mountains and outlet of the watershed respectively (Izady et al. 2015).
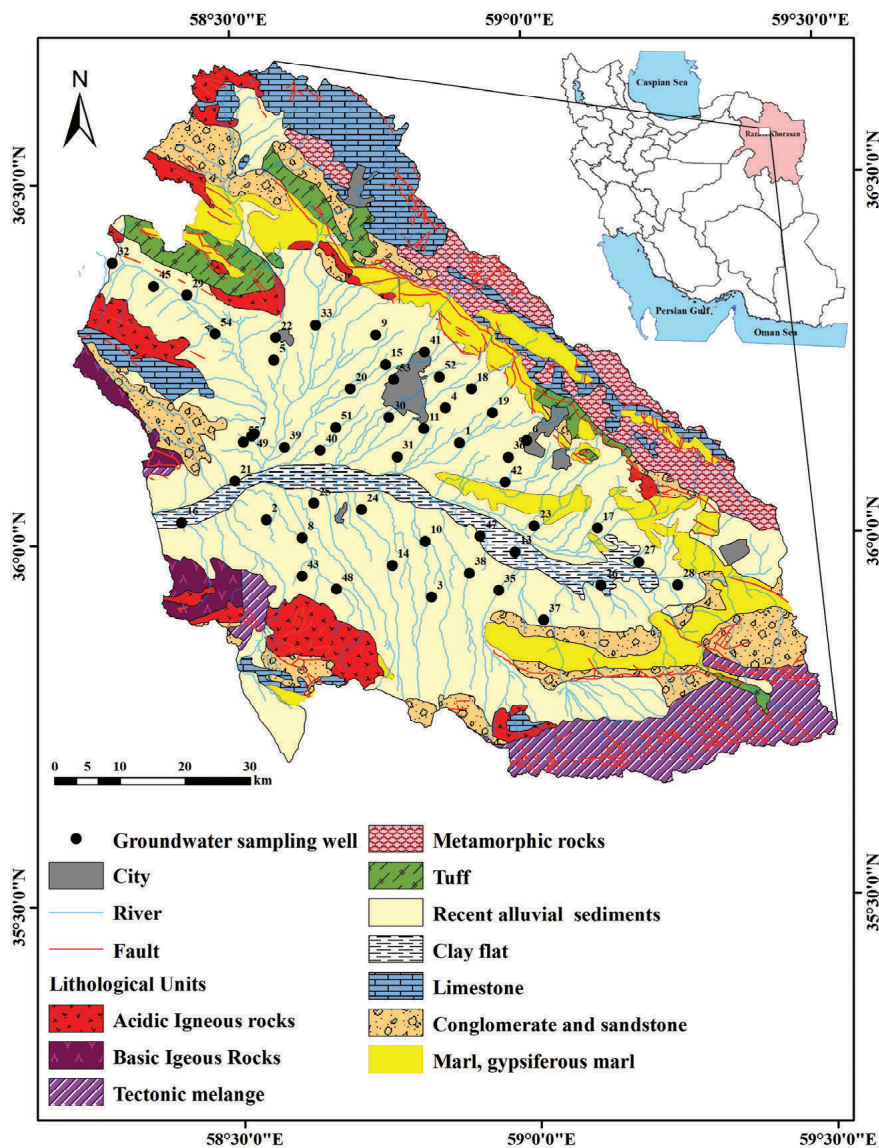

Fig. 1 - Geological map and groundwater sampling locations in the Neyshabour Plain (modified after Afshar Harb et al. 1987).

Fig. 1 - Carta geologica e posizione dei pozzi campionati nella pianura di Neyshabour (modificata da Afshar Harb et al. 1987).

Geology

The study area is located in the Binaloud-Central Iran Zones (Stocklin 1968; Dehghani et al. 2009). The main lithological units in the east and south east of the watershed include metamorphic rocks, limestone, gypsyferous marl, conglomerate, sandstone and ophiolitic mélanges with ages differing from Paleozoic to Cenozoic. Eocene volcano-sedimentary rocks and basic and acidic igneous rocks are the dominant lithological units formed in the mountainous areas to the west and north of the watershed (Afshar Harb et al. 1987) (Fig. 1). The Quaternary alluvial sediments cover low-elevation areas of the watershed hosting an alluvial aquifer (Dehghani et al. 2009).

Hydrogeology

The Neyshabour alluvial aquifer can be considered as a one-layer unconfined aquifer composed of Quaternary alluvial deposits with an area of 2833 km^2 (Izady et al. 2015). The alluvial aquifer is mostly recharged by subsurface inflow from mountainous area, irrigation return flow and precipitation. The general groundwater flow direction is from south-east and north towards west of the plain (Fig. 2).

Due to extensive development of agricultural activities and rapid population growth, the number of drilled wells has increased significantly from 306 in 1968 to 4462 in 2009. Overexploitation of groundwater resources in the study area led to continuous decline of groundwater levels which caused land subsidence (Dehghani et al. 2009; Izady et al. 2015; Dehghani and Nikoo 2019).

The extracted groundwater from Neyshabour alluvial aquifer is used for agricultural (82.8%) and industrial activities (16.1%) as well as drinking purposes (1.1%) (IWRMO 2017).

Sampling and analytical methods

Groundwater samples were taken from 55 wells in the study areas in May 2018. The location of the sampling points (wells) is shown in Figure 1. All samples were taken from deep pumping wells in different parts of the aquifer. All wells have long screen length that penetrates the full thickness of the Neyshabour aquifer. Groundwaters were sampled from each well after pumping for more than 15–30 min before sampling to remove the stagnant water and ensure that the collected water could accurately reflect the status of local groundwater (Zhai et al. 2017). Water samples were collected
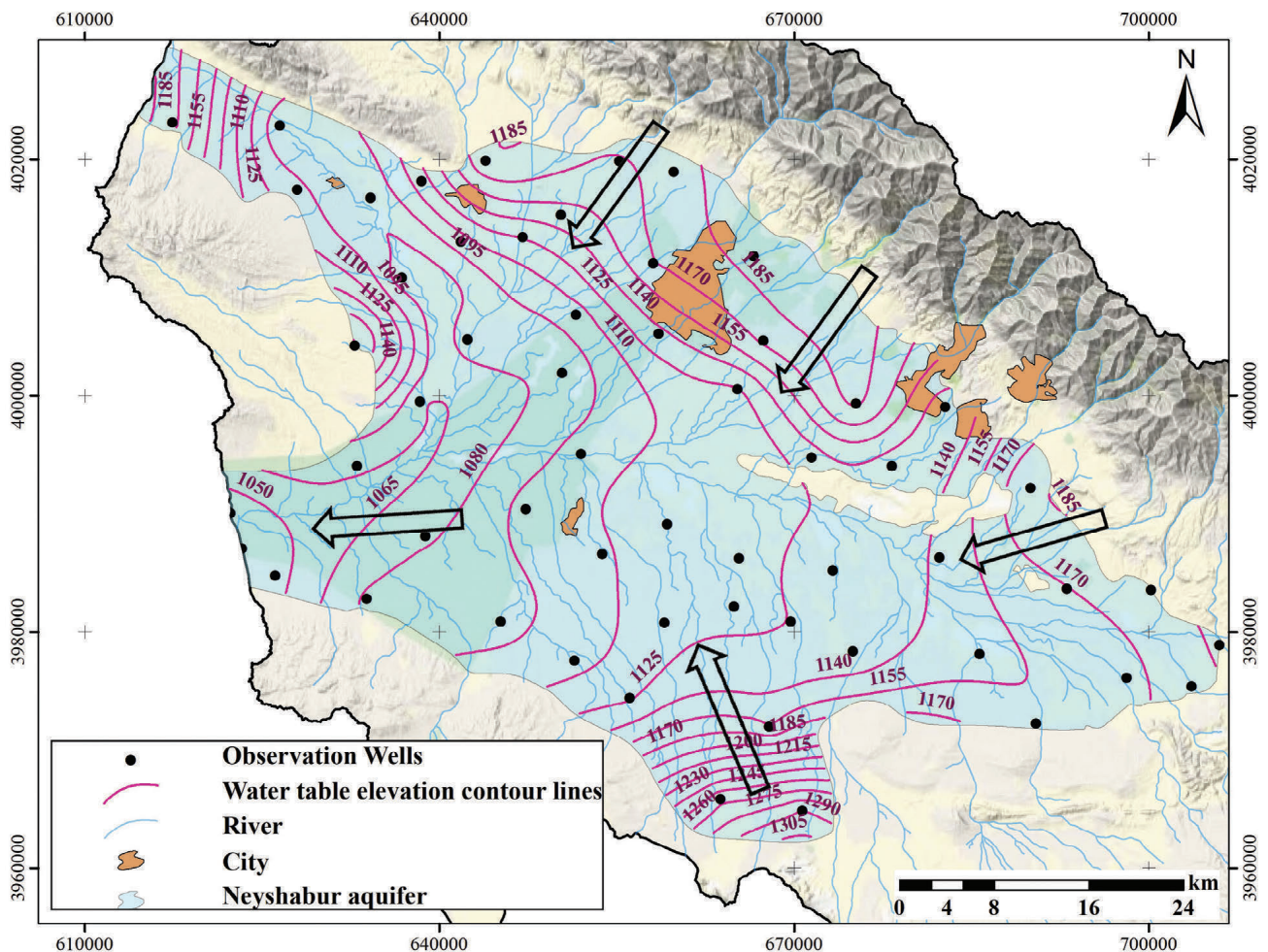

Fig. 2 - Water table contour map and the direction of groundwater flow in Neyshabour alluvial aquifer. The black arrows show groundwater flow direction.

Fig. 2 - Carta ad isopotenziali e direzioni prevalenti di flusso nell'acquifero alluvionale di Neyshabour. Le frecce nere indicano le direzioni di flusso.

and stored in pre-rinsed low-density polyethylene bottles. Electrical conductivity (EC), pH and temperature of water were measured on-site using portable instruments. Two samples were taken from each well. One sample was filtered and then acidified for cations analysis. The second sample was left unacidified for major anion analysis.

The chemical analyses of water samples were in accordance with American Public Health Association standard methods (APHA 2017). Sodium and potassium were analyzed using a flame photometer; bicarbonate and total alkalinity (TA) as $CaCO_3$ were measured using acid titration method; chloride concentration was measured by $AgNO_3$ titration method. Sulfate was determined by $BaCl_2$ turbidity method using a spectrophotometer. Ca^{2+}, Mg^{2+} and total hardness (TH) as $CaCO_3$ were analyzed using titration with EDTA. Analytical precision and measurement reproducibility were less than 2%. The obtained ionic balance was within 5%, which is considered acceptable for the hydrogeochemical characterizations.

The calculations of hydrogeochemical properties and creating the water chemistry diagrams were done using AqQA software. SPSS ver.22 and Excel 2013 software were used to statistical analysis.

Results and Discussion
General hydrogeochemistry

Statistical properties of the concentration of major ions, EC and pH are presented in Table 1 compared with acceptable values suggested by World Health Organization standards (WHO 2011) and Institute of Standards and Industrial Research of Iran (ISIRI 2010) for drinking water. The general trend of cations is $Na^+ >> Ca^{2+} > Mg^{2+} >> K^+$, while the dominance of anions is $Cl^- >> SO_4^{2-} >> HCO_3^-$. Figure 3 shows the boxplot diagram of studied parameters in Neyshabour Plain. The mean concentration of
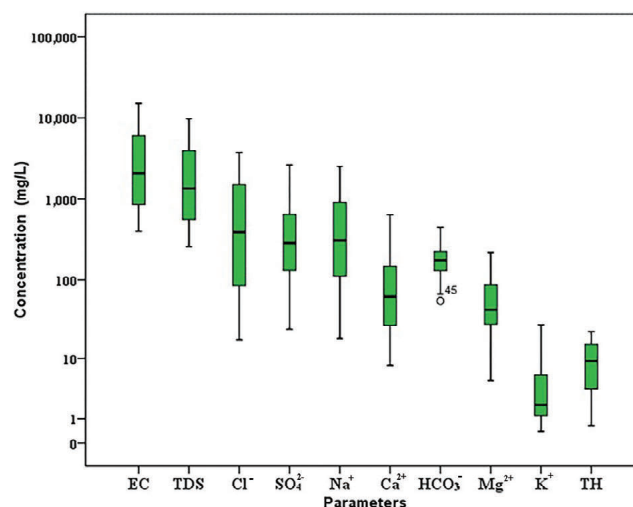

Fig. 3 - *Boxplot diagram shows the concentration of some physicochemical parameters in groundwater sample.*
Fig. 3 - Il diagramma boxplot mostra la concentrazione di alcuni parametri fisico-chimici nelle acque analizzate.

Mg^{2+} (61.4 mg/L), Na^+ (553.2 mg/L), Cl^- (800.4 mg/L) and SO_4^{2-} (428.7 mg/L) in groundwater samples are higher than WHO and ISIRI guideline values. Generally, the concentration of these parameters is increased toward discharge areas in the west of Neyshabour plain probably due to higher rate of residence time (Oinam et al. 2011; Tirkey et al. 2017).

The mean values of EC and TDS are 3404 µS/cm and 2212.8 mg/L, respectively, which both are higher than WHO standards. EC in 60% of samples and TDS in 85% of samples show EC value higher than permissible levels of WHO (2011). (Table 1). Higher salinity values are observed in the discharge area in the western part of the plain (Fig. 4a). pH value varies from 7.04 to 8.90 with mean value of 7.76 demonstrating weakly alkaline to alkaline water and is acceptable for

Tab. 1 - *Statistical properties of physicochemical parameters in the groundwater samples.*
Tab. 1 - Analisi statistica dei parametri fisico-chimici delle acque analizzate.

Parameter	Unit	Minimum	Maximum	Median	Mean	Std.	ISIRI[e]	WHO[f]
pH	-	7.04	8.90	7.77	7.76	0.34	6.5-9.0	6.5-7.5
EC[a]	µS/cm	399.0	14940.0	2080.0	3404.33	3196.25	-	1500
TDS[b]	mg/L	259.3	9711.0	1352.0	2212.81	2077.56	1000	500
Ca^{2+}	mg/L	8.02	641.20	62.12	109.19	127.50	300	200
Mg^{2+}	mg/L	4.86	218.70	42.53	61.40	46.09	30	50
K^+	mg/L	0.39	27.37	1.96	4.39	5.31	-	12
Na^+	mg/L	18.3	2529.0	310.40	553.20	560.35	200	200
HCO_3^-	mg/L	54.92	451.5	176.90	187.16	78.04	-	500
Cl^-	mg/L	17.73	3723.00	390.0	800.47	900.75	250	250
SO_4^{2-}	mg/L	24.02	2642.00	288.2	428.73	454.05	250	250
SAR[c]		0.62	22.36	9.15	9.59	6.78	-	-
TH[d]	mg/L	65.00	2500.00	315.0	525.09	485.32	500	500

[a] Electrical conductivity; [b] Total dissolved solids; [c] Sodium adsorption ratio; [d] Total hardness;
[e] Institute of Standards and Industrial Research of Iran (2010) acceptable value for drinking water;
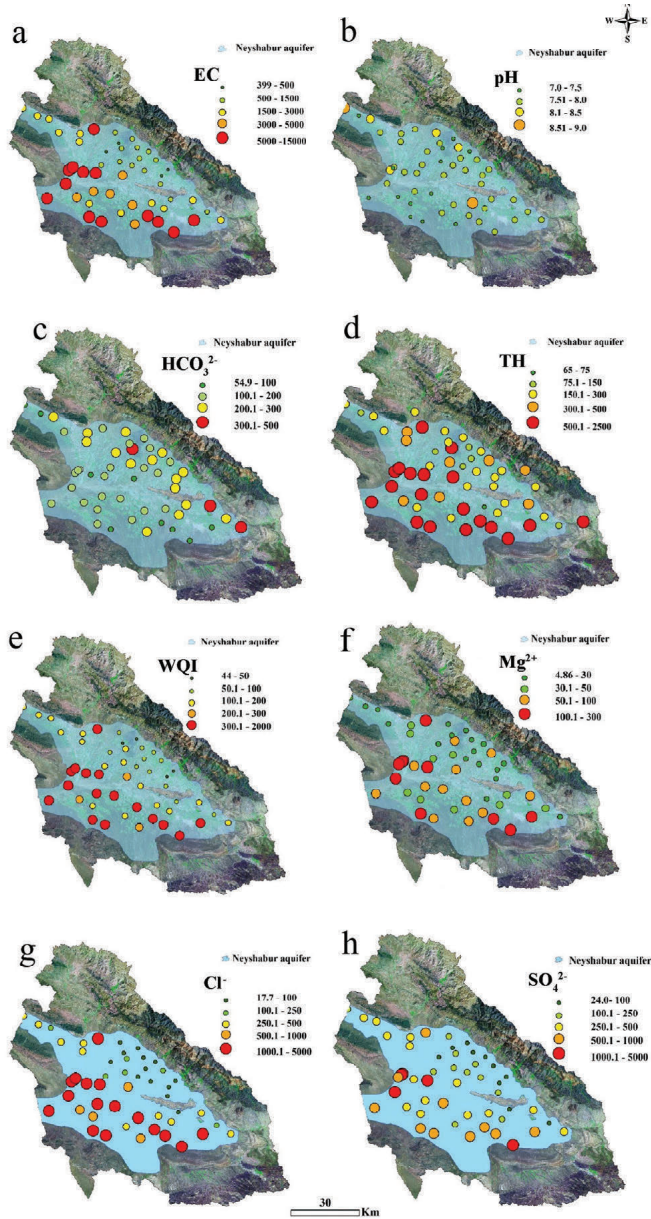[f] World Health Organization (2011) acceptable value for drinking water.

Fig. 4 - Distribution map of different physico-chemical parameters in Neyshabour aquifer.

Fig. 4 - Distribuzione di differenti parametri fisico-chimici nell'acquifero di Neyshabour.

Groundwater type

Piper diagram (Piper 1953) is commonly used to assess the water types and groundwater hydrogeochemical evolution based on the proportions of the major ions (Bouderbala 2015). The Piper diagram for studied samples reveals that Na-Cl is the dominant water type in the area (63.6 %) followed by Na-HCO$_3$ (14.5%) and Mg-HCO$_3$ (12.7%) type waters (Fig.5a). On the basis of this diagram, the groundwater samples can be divided into two general groups. Group 1 is situated in the center of the diamond-shape diagram comprises Na-HCO$_3$ and Mg-HCO$_3$ type waters which are distributed in the aquifer recharge areas. Group 2 which occupies the section near the right corner of Piper diagram includes Na-Cl type, mainly saline, waters which are mostly located in the middle and western parts of the aquifer (Fig. 5a). The plot of average chemical content of all samples on the Stiff diagram (Fig. 5b) shows the general trend of hydrogeochemical composition of water samples. It is indicated that Na and Cl are the dominant cation and anion in the groundwater samples, respectively.
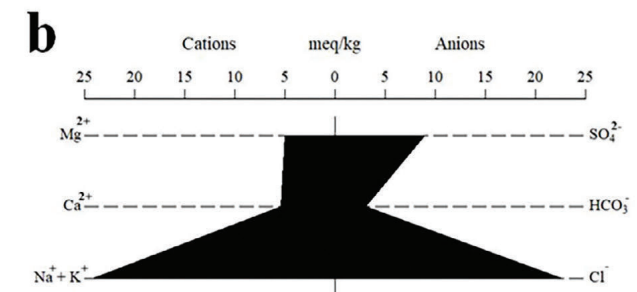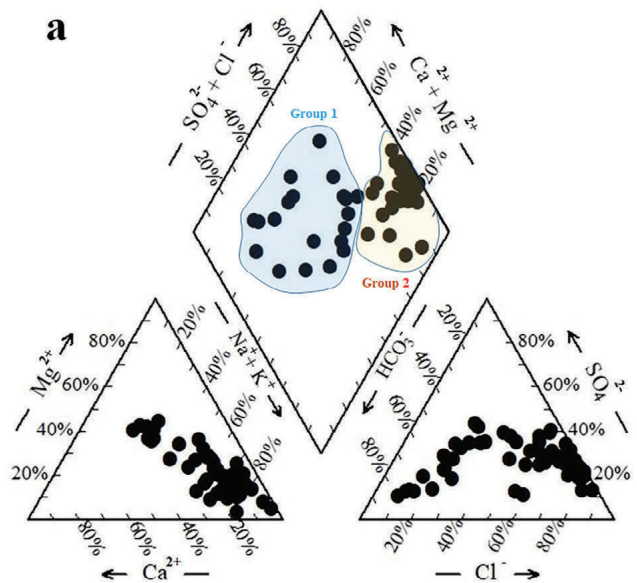
Fig. 5 - a) Piper diagram (Piper 1945) showing the chemical composition of groundwater samples of Neyshabour Plain. b) Stiff diagram demonstrates the average composition of groundwater samples.

Fig. 5 - a) Il diagramma di Piper (Piper 1945) mostra la composizione chimica delle acque sotterranee nella pianura di Neyshabour. b) Il diagramma di Stiff mostra la composizione media delle acque analizzate.

drinking on the basis of WHO and ISIRI guidelines. Higher pH values are observed in the samples which are located in center and north of the plain (Fig. 4b). The maximum HCO$_3^-$ contents are observed in the samples located in the east of the plain (Fig. 4 c). The majority of parameters such as Mg^{2+}, Cl$^-$ and SO$_4^{2-}$ show maximum values in the central and west of the plain (Fig. 4).

TH values of the samples range from 65.0 to 2500.0 mg/L, with an average value of 525.0 mg/L (Tab. 1). Regarding TH values, 36.3% of the samples fell higher than ISIRI maximum allowable limit (500 mg/L). Considering hardness classification of Sawyer et al. (2003), the groundwater samples are very hard to hard waters (Tab. 2).

Hydrogeochemical factors affecting groundwater chemistry

Chemical weathering and dissolution

Gibbs's diagram (Gibbs 1970) was used to assess the sources of major ions in the groundwater samples. The distribution of sample data points on this diagram suggests that rock weathering and evaporation/evaporate dissolution are the most important factors influencing the groundwater quality in Neyshabour aquifer (Fig. 6a).

The plot of Na-normalized Ca^{2+} versus Mg^{2+} (Gaillardet et al. 1999) (Fig. 6b) suggests that the water samples are influenced by silicate weathering and evaporites dissolution which is consistent with the dominance of Na-Cl and Na-HCO_3 type waters in the area.

The plot of $Na^+ + K^+$ against Cl^- (Fig. 6c) shows that high TDS samples fall near 1:1 line indicating the dissolution of evaporate minerals. These samples are distributed in the discharge zones in the west of the Neyshabour plain. An excess of $Na^+ + Cl^-$ over Cl^- (i.e. >1.5) in the samples located in recharge areas suggesting other sources of the alkalis, e.g., the weathering of silicate minerals and/or cation exchange (Yang

et al. 2020). In the diagram of $Ca^{2+} + Mg^{2+}$ versus HCO_3^- (Fig. 6d) the majority of samples falls on the top of 1:1 line suggesting the input of Ca and Mg from non-carbonate sources such as silicate weathering, dissolution of evaporite minerals or reveres ion exchange (Kumar et al. 2015). The similar pattern was observed in the diagram of $Ca^{2+} + Mg^{2+}$ versus $HCO_3^- + SO_4^{2-}$ (Fig. 6e).

Mg^{2+}/Ca^{2+} ratio values greater than 1 in fresh water could be the result of water interacting with Mg-rich silicate rocks such as olivine bearing volcanic rocks (Schoeller 1956; Hem 1985). In the Neyshabour plain 58.1% of samples show $Mg^{2+}/Ca^{2+}>1$. This is probably due to the chemical weathering of mafic and ultramafic rocks such as dunite in ophiolitic series in the southern part of the study area.

Ion exchange

In cation exchange, Na^+ on the exchangeable sites of the clay minerals can be replaced by Mg^{2+} and Ca^{2+} of groundwater, resulting in the increase of Na^+ and decrease of Ca^{2+} and Mg^{2+} in groundwaters which could be represented by the following reaction:
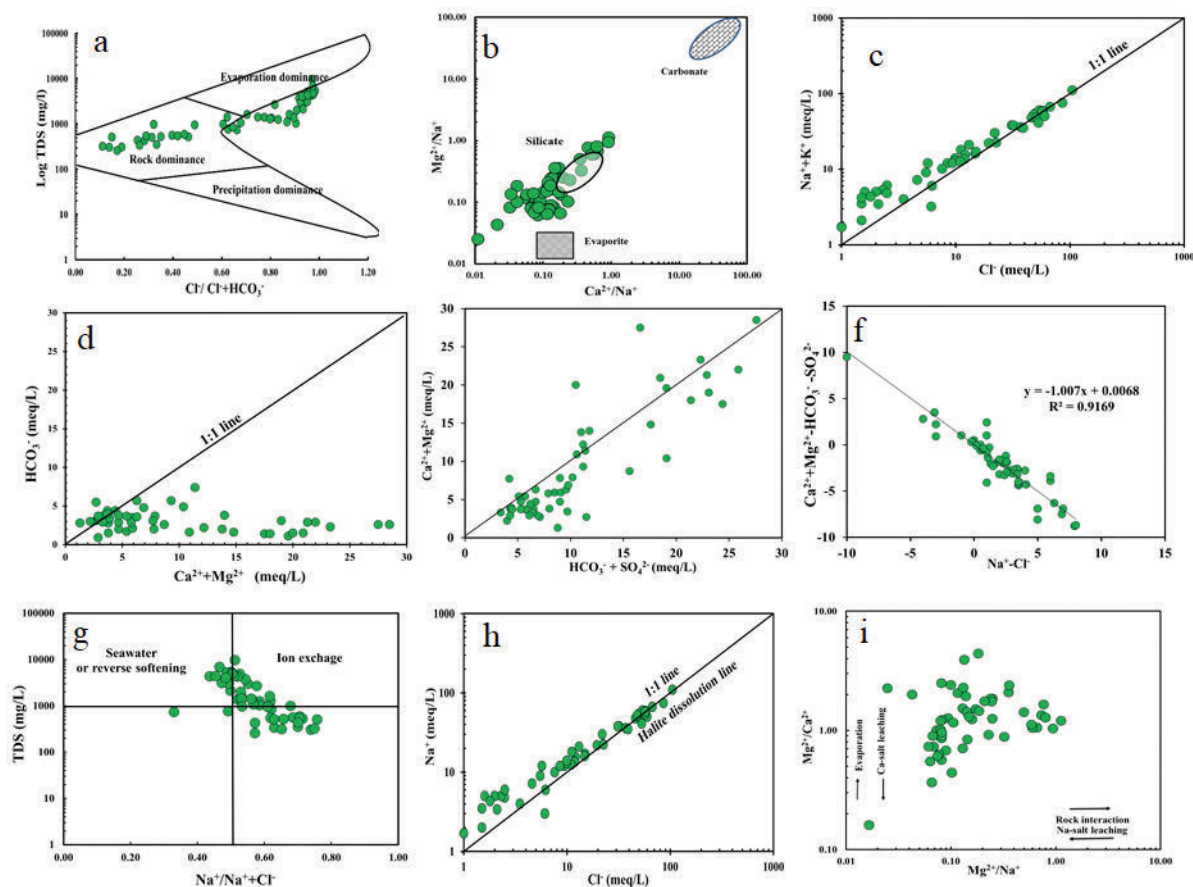
$$\text{Na-Clay} + \tfrac{1}{2}\,Ca^{2+} \longrightarrow Na^+ + \tfrac{1}{2}\,\text{Ca-Clay}_2 \qquad (1)$$

Fig. 6 - Plots of a) Gibbs (1970) diagram; b) Mg^{2+}/Ca^{2+} versus Ca^{2+}/Na^+ (Gaillardet et al. 1999); c) $Na^+ + K^+$ versus Cl^-; d) HCO_3^- versus $Ca^{2+} + Mg^{2+}$; e) $Ca^{2+} + Mg^{2+}$ versus $HCO_3^- + SO_4^{2-}$; f) $Ca^{2+} + Mg^{2+} - HCO_3^- + SO_4^{2-}$ versus $Na^+ - Cl^-$; g) TDS versus $Na^+/Na^+ + Cl^-$; h) Na^+ versus Cl^-; i) molar ratios of Mg^{2+}/Ca^{2+} versus Mg^{2+}/Na^+ (Webster et al. 1994; Priestley et al. 2020).

Fig. 6 - Diagrammi di a) Gibbs (1970); b) Mg^{2+}/Ca^{2+} contro Ca^{2+}/Na^+ (Gaillardet et al. 1999); c) $Na^+ + K^+$ contro Cl^-; d) HCO_3^- contro $Ca^{2+} + Mg^{2+}$; e) $Ca^{2+} + Mg^{2+}$ contro $HCO_3^- + SO_4^{2-}$; f) $Ca^{2+} + Mg^{2+} - HCO_3^- + SO_4^{2-}$ contro $Na^+ - Cl^-$; g) TDS contro $Na^+/Na^+ + Cl^-$; h) Na^+ contro Cl^-, i. rapporto molare di Mg^{2+}/Ca^{2+} contro Mg^{2+}/Na^+ (Webster et al. 1994; Priestley et al. 2020).

Cation exchange in an aquifer system can be proved by the plot of $Ca^{2+} + Mg^{2+} - HCO_3^- + SO_4^{2-}$ versus $Na^+ - Cl^-$ (Naderi et al. 2020). The samples affected by the cation exchange process are placed on a line with a slope of -1.0 (Singh et al. 2013). Figure 6f illustrates that groundwater samples followed a straight line ($R^2 = 0.91$) suggesting that Na^+, Ca^{2+} and Mg^{2+} are involved in the ion exchange reaction. The ion exchange is confirmed by the plotting of data on the diagram of TDS versus $Na^+/Na^+ + Cl^-$ (Fig. 6g) indicating the occurrence of ion exchange in more than 6% of samples.

Origin of Salts in Groundwater

Richter and Kreitler (1993) defined water salinization as an increase in total dissolved solids (TDS). Generally, salinity increases along groundwater flow paths from recharge to discharge area (Richter and Kreitler 1993, Dehbandi et al. 2019).

The diagram of Na^+ versus Cl^- can be used to identify the mechanism salinity in groundwater (Priestley et al. 2020). High contents of Na^+ and Cl^- in the groundwater samples may be originated from evaporite mineral dissolution. Equal concentrations of Na^+ and Cl^- are released by dissolution of halite (Pauloo et al. 2021). In the plot of Na versus Cl^- (Fig. 6h) samples with high TDS are plotted near 1:1 line indicative of halite dissolution. These samples are close to watershed discharge zone. However, Na^+/Cl^- molar ratio in the majority of samples (67%) is higher than unity (average = 1.4). This indicates that there are other sources of Na such as silicate weathering or cation exchange (Yang et al. 2020).

Webster et al. (1994) introduced the ratios of Mg^{2+}/Na^+ and Mg^{2+}/Ca^{2+} as an indication of the soil salt leaching and evaporation in arid environments. In the diagram of Mg^{2+}/cations (Figure 6i) the majority of samples show high Mg^{2+}/Ca^{2+} ratios, indicating that evaporation and rock interaction appears to be more important process rather than salt-leaching in the study area.

It can be concluded, rock-water reactions including evaporites dissolution is the main source of the salinity in the study area. Most extracted groundwater is used for irrigation. Crop transpiration and evaporation increase the return flows salinity relative to the applied irrigation water (Pulido-Bosch et al. 2018). Moreover, decline in water levels, caused by excessive groundwater withdrawal, can result in reducing natural groundwater outflow and accumulating salts in the groundwater system (Pauloo et al. 2021).

Cluster Analysis (CA)

Figure 7 indicates the result of CA on the samples which confirms the outcomes of correlation coefficients. On the basis of CA the variables can be classified to two main groups. Group 1 includes TH, SO_4^{2-}, Mg^{2+}, Na^+, Ca^{2+}, Cl^-, TDS and EC displaying the important roles of evaporation and evaporite dissolution on the enrichment of salts in groundwater. Group 2 comprises HCO_3^- and pH indicating the role of silicate minerals weathering and carbonate dissolution which are predominant events in the recharge areas as indicated in Figures 4e and 4d. Figure 4c indicates that high values of

HCO_3^- mostly occurs in the east and southeast of Neyshabour Plain which is regarded as recharge areas with dominant silicate rocks such as metamorphic and ophiolitic series in highland terrains in the east and southeast of the aquifer.
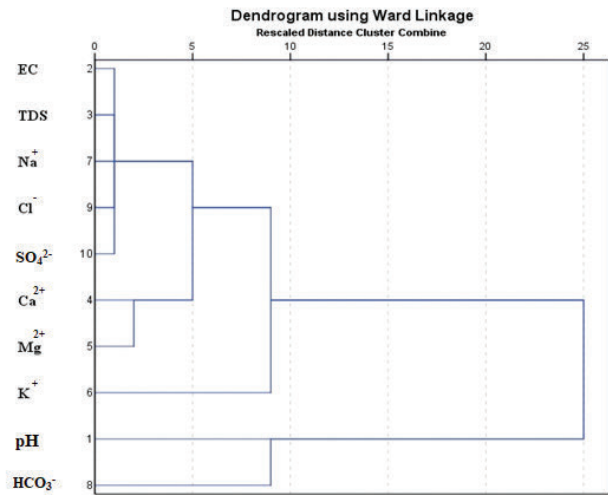

Fig. 7 - Hierarchical cluster using Ward's method with squared Euclidean distances between groups in studied groundwater samples.
Fig. 7 - Gerarchia di cluster ottenuta mediante il metodo di Ward e quadrato della distanza euclidea fra i gruppi delle acque analizzate.

Suitability of groundwater for drinking and agriculture purposes
Evaluation of Water Quality for Irrigation Purpose

There are some criteria based on chemical composition of groundwater to evaluate groundwater quality for irrigation and agricultural purposes. Table 2 displays some of these criteria and indices and their calculation equation including sodium percentage (Na%), residual sodium bi-carbonate (RSBC), permeability index (PI), sodium absorption ratio (SAR), magnesium adsorption ratio (MAR), Kelly's ratio (KR) and salinity.

Salinity hazard can be estimated by EC and considered as the most important water quality guideline on crop productivity (Ramesh and Elango 2012; Tomaz et al. 2020). Totally, 41.6% of samples show high salinity (EC> 2250 µS/cm) which are not suitable for irrigation (Tab. 2). These samples mostly are located in south, central and west of Neyshabour plain as indicated by Figure 4a. Sodium percentage (%Na) differs from 21.45% to 93.27% (Tab. 2). 67.2 % of samples show %Na values higher that maximum limit for irrigation water (%Na=60) which is recommended by WHO (2011). The values of %Na greater than 60 % may result in sodium accumulations in soils that will cause reduce in permeability and changes in the soil's physical properties (Wilcox 1955). Sodium hazard can also be assessed by Kelly Ratio (KR). From all samples 78.1% show KR higher than 1 indicating unsuitability of waters for irrigation. On the basis of this index, groundwater in the majority of Neyshabour Plain is not suitable for irrigation purposes except in the east and north of the plain.

The PI values vary from 44% to 99% (Tab. 2) indicating 52.7% of samples are classified as unsuitable and can affect soil permeability by long-term use for irrigation. Spatially, these samples do not show a regular distribution but mostly are located in south and center of Neyshabour Plain. MAR values in the studied samples ranged from 13.7% to 81.4%. More than 62% of samples show excess of magnesium and are unsuitable for agricultural purposes, because high values of magnesium affect the quality of soils and decreases crop yield (Joshi et al. 2009).

The Evaluation of Water Quality for drinking purpose

The Water Quality Index (WQI) has been widely used to evaluate the suitability of both surface water and groundwater quality for drinking purposes (Ramakrishnaiah et al. 2009; Aly et al. 2015; Herojeet et al. 2020). This index effectively converts numerous physical and chemical parameters into a single value to reflect the overall quality of water (Wu et al. 2017).

Each environmental parameter was assigned a weight according to the parameters' relative importance in the overall quality of water for drinking water purposes. A weight of 5 was assigned for TDS; 4 for Cl^-, EC, and SO_4^{2-}; 3 for pH, TH, HCO_3^-; 2 for Ca^{2+}, Na^+, and K^+ and 1 for Mg^{2+} (Logeshkumaran et al. 2015; Adimalla et al. 2018; Dehbandi et al. 2018). Several methods have been proposed to calculate WQI using different parameters over the world (Debels et al. 2005; Koçer and Sevgili 2016). The method proposed by Logeshkumaran et al. (2015) was used to calculate WQI. The relative weight (W_i) of each parameter is computed using following formula:

$$W_i = \frac{w_i}{\sum_{i=1}^{n} w_i} \qquad (2)$$

Where: w_i indicates the weight of each parameter, and n is the number of parameters.

The quality rating (Q_i) for each chemical parameter is calculated as follow:

$$Q_i = \frac{c_i}{s_i} 100 \qquad (3)$$

In this formula, C_i is the concentration of each chemical parameter in each water sample (mg/L) and S_i is the WHO standard of drinking water for each selected parameter (mg/L) (WHO 2011). Then, SI_i (the sub-index of ith parameter) is determined for each chemical parameter using the following equation:

$$SI_i = W_i \cdot Q_i \qquad (4)$$

Finally, WQI is determined as follow:

$$WQI = \sum_{i=1}^{n} SI_i \qquad (5)$$

The water quality can be categorized into five types based on the WQI scores: excellent (0–20), good (21–40), moderate (41–60), low (61–80), and bad (81–100) (Ramakrishnalah et al. 2009).

The results of WQI indicate that 32.6% of samples are grouped in excellent and good water, and 33% of samples are not suitable for drinking purposes. Nearly, 29 % of samples fell under poor water category and 5% are very poor water quality for drinking. Figure 4e shows that higher values of WQI are observed in south and west of the Neyshabour plain in accordance with TDS, Cl^-, Na^+ and EC distribution.

Moreover, the diagram of TDS versus TH (Richards 1954) (Fig. 8) displays a detailed classification of groundwater quality and confirms that almost 23.6 % of the samples are classified as very hard-brackish type waters, 21.8 % are slightly hard- brackish and 20% are very hard-freshwater types. Most of brackish waters were located in central and west of the Neyshabour Plain (Fig. 4d). It seems that water hardness in the studied area is permanent hardness due to presence of calcium, magnesium chlorides, and sulfates.
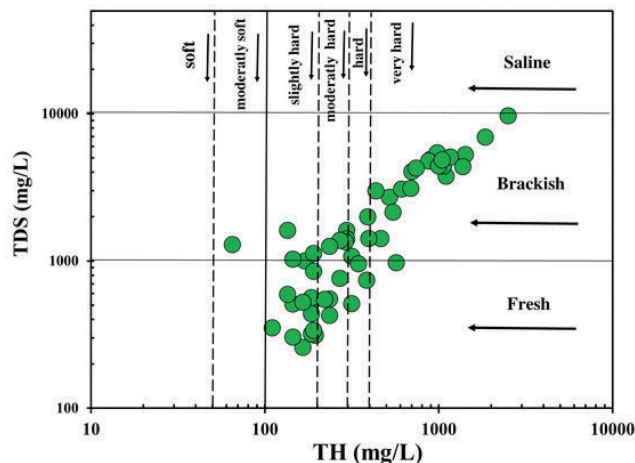

Fig. 8 - Diagram of TDS versus TH for assessing the natural water quality for drinking purposes (Richards 1954).
Fig. 8 - Diagramma TDS contro TH per determinare la qualità delle acque sotterranee per scopi idropotabili (Richards 1954).

Conclusion

This research used different hydrogeochemical methods and indices to evaluate the main controlling processes of groundwater chemistry as well as the groundwater quality for irrigation and drinking purposes in Neyshabour plain. Interpretation of analytical data showed that the major ions in the groundwater samples have the following trend in cations: $Na^+ \gg Ca^{2+} > Mg^{2+} \gg K^+$ and anions: $Cl^- \gg SO_4^{2-} \gg HCO_3^-$. The mean values of Na^+, Mg^{2+}, TDS, EC, TH, SO_4^{2-}, Cl^- are higher than Iranian national standard and WHO guideline. Na and Cl are the dominate cations and anions in wells near the discharge zones and Na^+-Cl^- is the dominant water type in the plain. Unfortunately, groundwater in most places in Neyshabour aquifer is not suitable for irrigation and drinking purposes. Whereas, the recharge areas in the east and north east parts of the aquifer are characterized by low

Tab. 2 - Classification of groundwater in the Neyshabour plain.
Tab. 2 - Classificazione delle acque sotterranee nella pianura di Neyshabour.

Classification pattern	Categories	Ranges	Number of samples	% of samples
Electrical conductivity (**EC**) (Wilcox 1955)	Excellent	<250	0	0
	Good	250–750	8	14.5
	Permissible	750–2,250	24	43.6
	Doubtful	2,250–5,000	8	14.4
	Unsuitable	>5,000	15	27.2
TH (Sawyer and McMcartly 1967)	Soft	<75	1	1.8
	Moderately high	75–150	6	10.9
	Hard	150–300	20	36.3
	Very hard	>300	28	50.9
Percent sodium (%Na) (Wilcox 1955) $Na\% = \dfrac{Na^+ + K^+}{Ca^{2+} + Mg^{2+} + K^+ + Na^+}$	Excellent	0–20	0	0
	Good	20–40	8	14.5
	Permissible	40–60	10	18.1
	Doubtful	60–80	33	60.0
	Unsuitable	>80	4	7.2
Sodium absorption ratio (SAR) (Richard 1954) $SAR = \dfrac{Na^+}{\sqrt{\dfrac{Ca^{2+} + Mg^{2+}}{2}}}$	Very low	<2	9	16.3
	Low	2–12	27	49.0
	Medium	12–22	17	30.9
	High	22–32	2	3.6
	Very high	32	0	0
Permeability index (PI) (Doneen 1964) $PI = \dfrac{Na^+ + \sqrt{HCO_3^-}}{Na^+ + Mg^{2+} + Ca^{2+}} \times 100$	Suitable	<75	25	45.4
	Unsuitable	75≥	30	54.6
Residual sodium bi-carbonate (RSBC) (meq/L) $RCS = \left(HCO_3^- + CO_3^{2-}\right) - \left(Ca^{2+} + Mg^{2+}\right)$ (Eaton 1950 and Richards 1954)	Permissible	<5	55	100
	Unsuitable	5≥	0	0
Magnesium adsorption ratio (MAR) (Raghunath 1987) $MAR = \dfrac{Mg^{2+}}{Ca^{2+} + Mg^{2+}} \times 100$	Permissible	0–50	18	32.7
	Unsuitable	>50	37	62.7
Kelly's ratio (Kelly 1940) $KR = \dfrac{Na^+}{Mg^{2+} + Ca^{2+}}$	Suitable	<1	12	21.8
	Unsuitable	≥1	43	78.1
WQI	Excellent water	<50	1	1.8
	Good water	50-100	17	30.9
	Poor water	100-200	15	27.2
	Very poor water	200-300	4	7.2
	Unsuitable for drinking purposes	>300	18	32.7

salinity and the groundwater is suitable for drinking and agricultural purposes. Groundwater salinization threatens drinking water supply and agricultural productivity in this area.

The combination of multivariate statistical approaches and geochemical methods revealed that total dissolved solids in groundwater is mainly affected by combination of rock-water reactions including evaporites dissolution and ion exchange in Neyshabour aquifer. Moreover, irrigation return flows and groundwater level decline, caused by excessive groundwater withdrawal for agricultural use (82.8% of total groundwater extraction), intensified groundwater salinity. Further studies are needed for partitioning salinization processes between rock-water reactions and irrigation return flows.

Competing interest
The authors declare no competing interest.

Additional information
Supplementary information is available for this paper at
https://doi.org/10.7343/as-2021-502
Reprint and permission information are available writing to
acquesotterranee@anipapozzi.it
Publisher's note Associazione Acque Sotterranee remains neutral with regard to jurisdictional claims in published maps and institutional affiliations.

REFERENCES

Afshar Harb A, Aghanabati A, Majidi B, Alavi Tehrani. N (1987) Geological quadrangle map of Iran, No. K4 (Mashhad), Scale 1:250000. Geological Survey of Iran, Tehran.

Adimalla N, Li P, Venkatayogi S (2018) Hydrogeochemical evaluation of groundwater quality for drinking and irrigation purposes and integrated interpretation with water quality index studies. Environmental Processes. 5(2), 363-383.

Aly A, Al-Omran AM, Alharby M (2015) The water quality index and hydrochemical characterization of groundwater resources in Hafar Albatin, Saudi Arabia. Arabian Journal of Geosciences, 8(6), 4177-4190.

APHA (2017) Standard Methods for the Examination of Water and Wastewater. 23th ed. American Public Health Association. Washington.

Bouderbala A (2015) Assessment of groundwater quality and its suitability for agricultural uses in the Nador Plain, north of Algeria. Water Quality. Exposure and Health. 7(4): 445-457.

Debels P, Figueroa R, Urrutia R, Barra R, Niell X (2005) Evaluation of water quality in the Chillán River (Central Chile) using physicochemical parameters and a modified water quality index. Environmental monitoring and assessment 110(1-3): 301-322.

Dehbandi R, Moore F, Keshavarzi B, Abbasnejad A (2017) Fluoride hydrogeochemistry and bioavailability in groundwater and soil of an endemic fluorosis belt, central Iran. Environmental Earth Sciences. 76(4): 177.

Dehbandi R, Moore F, Keshavarzi B (2018) Geochemical sources, hydrogeochemical behavior. and health risk assessment of fluoride in an endemic fluorosis area, central Iran. Chemosphere. 193: 763-776.

Dehbandi R, Abbasnejad A, Karimi Z, Herath I, Bundschuh J (2019) Hydrogeochemical controls on arsenic mobility in an arid inland basin, Southeast of Iran: The role of alkaline conditions and salt water intrusion. Environmental Pollution. 249: 910-922.

Dehghani M, Valadan Zoej MJ, Entezam I, Mansourian A, Saatchi S (2009) InSAR monitoring of progressive land subsidence in Neyshabour, northeast Iran. Geophysical Journal International. 178(1) 47-56.

Dehghani M, Nikoo MR (2019) Monitoring and Management of Land Subsidence Induced by Over-exploitation of Groundwater. In Natural Hazards GIS-Based Spatial Modeling Using Data Mining Techniques 271-296. Springer. Cham.

Doneen L (1964) Notes on water quality in Agriculture Published as a Water Science and Engineering Paper 4001. Department of water science and Engineering, University of California.

Gaillardet J, Dupré B, Louvat P, Allegre CJ (1999) Global silicate weathering and CO_2 consumption rates deduced from the chemistry of large rivers. Chemical geology 159(1-4) 3-30.

Giambastiani BM, Colombani N, Mastrocicco M, Fidelibus MD (2013) Characterization of the lowland coastal aquifer of Comacchio (Ferrara, Italy): hydrology, hydrochemistry and evolution of the system. Journal of Hydrology 501: 35-44.

Gibbs R J (1970) Mechanisms controlling world water chemistry. Science. 170(3962), 1088-1090.

Hem JD (1985) Study and interpretation of the chemical characteristics of natural water. 3rd Edn. U.S. Geol. Surv. Water Supply 2254.

Herojeet R, Naik PK, Rishi MS (2020) A new indexing approach for evaluating heavy metal contamination in groundwater, Chemosphere 245. https://doi.org/10.1016/j.chemosphere.2019.125598.

Institute of Standards and Industrial Research of Iran (ISIRI) (2010) Drinking Water physical and Chemical Specifications (1053). 5th revision, Institute of Standards and Industrial Research of Iran.

Iranian Water Resources and Management Organization (IWRMO) (2017) Final report of groundwater resources in Neyshabour Basin. Internal report (In Farsi with English abstract).

Izady A, Davary K, Alizadeh A (2015) Groundwater conceptualization and modeling using distributed SWAT-based recharge for the semi-arid agricultural Neyshabour plain. Iran. Hydrogeol J 23. 47–68. https://doi.org/10.1007/s10040-014-1219-9.

Joodavi A, Izady A, Karbasi Maroof MT, Majidi M, Rossetto R (2020) Deriving optimal operational policies for off-stream man-made reservoir considering conjunctive use of surface- and groundwater at the Bar dam reservoir (Iran), Journal of Hydrology: Regional Studies 31, 100725. https://doi.org/10.1016/j.ejrh.2020.100725.

Joshi DM, Kumar A, Agrawal N (2009) Assessment of the irrigation water quality of river Ganga in Haridwar district. Rasayan J Chem 2(2): 285-292.

Kelly W (1940) Permissible composition and concentration of irrigated waters. Paper presented at the Proceedings of the ASCF.

Koçer MAT, Sevgili H (2014) Parameters selection for water quality index in the assessment of the environmental impacts of land-based trout farms. Ecological Indicators 36: 672-681.

Kumar PS, Jegathambal P, Nair S, James EJ (2015) Temperature and pH dependent geochemical modeling of fluoride mobilization in the groundwater of a crystalline aquifer in southern India. Journal of Geochemical Exploration 156: 1-9.

Logeshkumaran A, Magesh NS, Godson PS, Chandrasekar N (2015) Hydro-geochemistry and application of water quality index (WQI) for groundwater quality assessment. Anna Nagar. part of Chennai City. Tamil Nadu, India. Applied Water Science 5(4): 335-343.

Mirzavand M, Sadeghi SH, Bagheri R (2020) Delineating the source and mechanism of groundwater salinization in crucial declining aquifer using multi-chemo-isotopes approaches. Journal of Hydrology 586. https://doi.org/10.1016/j.jhydrol.2020.124877.

Naderi M, Jahanshahi R, Dehbandi R (2020) Two distinct mechanisms of fluoride enrichment and associated health risk in springs' water near an inactive volcano. southeast Iran. Ecotoxicology and Environmental Safety 19(5): 110503.

Oinam J.D, Ramanathan A L, Linda A, Singh G (2011) A study of arsenic, iron and other dissolved ion variations in the groundwater of Bishnupur District. Manipur, India. Environmental Earth Sciences. 62(6): 1183-1195.

Pauloo RA, Fogg GE, Guo Z, Harter T (2021) Anthropogenic basin closure and groundwater salinization (ABCSAL), Journal of Hydrology 593, 125787. https://doi.org/10.1016/j.jhydrol.2020.125787.

Priestley SC, Shand P, Love AJ et al. (2020) Hydrochemical variations of groundwater and spring discharge of the western Great Artesian Basin, Australia: implications for regional groundwater flow. Hydrogeol J 28, 263–278. https://doi.org/10.1007/s10040-019-02071-3.

Pulido-Bosch A, Rigol-Sanchez JP, Vallejos A et al. (2018) Impacts of agricultural irrigation on groundwater salinity. Environ Earth Sci 77, 197. https://doi.org/10.1007/s12665-018-7386-6

Raghunath H (1987) Groundwater (2nd ed.). Delhi India: Wiley Eastern Ltd.

Richards LA (1954) Diagnosis and improvement of saline and alkali soils. Soil Sci. 7(8).15-23.

Richter BC, Kreitler CW (1993) Geochemical techniques for identifying sources of groundwater salinization. United States of America, Library of Congress Cataloging-in-publication Data.

Sawyer CN, McCarty PL, Parkin G F (1994) Chemistry for environmental engineering (Vol. 4). New York: McGraw-Hill.

Schoeller H (1956) Geochemie des eaux souterraines. Application aux eaux des gisements de petrole. Soc. Ed. Technip, Paris. 213

Narany TS, Ramli MF, Aris AZ, Sulaiman WNA, Fakharian K (2014) Spatiotemporal variation of groundwater quality using integrated multivariate statistical and geostatistical approaches in Amol–Babol Plain. Iran. Environmental monitoring and assessment. 186(9): 5797-5815.

Ramakrishnaiah CR, Sadashivaiah C, Ranganna G (2009) Assessment of water quality index for the groundwater in Tumkur Taluk, Karnataka State. India. E-Journal of chemistry 6.

Ramesh K, Elango L (2012) Groundwater quality and its suitability for domestic and agricultural use in Tondiar river basin. Tamil Nadu. India. Environmental monitoring and assessment 184(6): 3887-3899.

Singh AK, Raj B, Tiwari AK et al. (2013) Evaluation of hydrogeochemical processes and groundwater quality in the Jhansi district of Bundelkhand region, India. Environ Earth Sci 70, 1225–1247. https://doi.org/10.1007/s12665-012-2209-7

Stocklin J (1968) Structural history and tectonics of Iran: a review. AAPG Bull. 5(2):1229-1258

Tirkey P, Bhattacharya T, Chakraborty S, Baraik S (2017) Assessment of groundwater quality and associated health risks: a case study of Ranchi city. Jharkhand. India. Groundwater for Sustainable Development 5: 85-100.

Tomaz A, Palma P, Alvarenga P, Gonçalves MC (2020) Soil salinity risk in a climate change scenario and its effect on crop yield. In Climate Change and Soil Interactions 351-396. Elsevier.

Webster JG, Brown KL, Vincent WF (1994) Geochemical processes affecting meltwater chemistry and the formation of saline ponds in the Victoria Valley and Bull Pass region. Antarctica. Hydrobiologia 281(3): 171-186.

WHO (2011) Guidelines for Drinking-Water Quality. 4th edition. World Health Organization. Geneva. Switzerland.

Wilcox LV (1955) Classification and use of irrigation water. Agric circ 969. USDA. Washington D.C. p 19

Wu Z, Wang X, Chen Y, Cai Y, Deng J (2018) Assessing river water quality using water quality index in Lake Taihu Basin, China. Science of the Total Environment 612: 914-922.

Yang J, Ye M, Tang Z, Jiao T, Song X, Pei Y, Liu H (2020) Using cluster analysis for understanding spatial and temporal patterns and controlling factors of groundwater geochemistry in a regional aquifer. Journal of Hydrology 583, 124594. https://doi.org/10.1016/j.jhydrol.2020.124594

Zhai Y, Zhao X, Teng Y, Li X, Zhang J, Wu J, Zuo R (2017) Groundwater nitrate pollution and human health risk assessment by using HHRA model in an agricultural area. NE China. Ecotoxicology and environmental safety 137: 130–142. https://doi.org/10.1016/j.ecoenv.2016.11.010